Beyond Lux: Methods for Species and Photoreceptor-Specific Quantification of Ambient Light for Mammals

Richard J McDowell [1*], Altug Didikoglu [1,2*], Tom Woelders [1], Mazie J Gatt [1], Roelof A Hut[3] Timothy M Brown [4], Robert J Lucas [1#]

[1] Centre for Biological Timing, Division of Neuroscience, School of Biological Sciences, Faculty of Biology Medicine and Health, University of Manchester, Manchester M13 9PT, UK

[2] Department of Neuroscience, Izmir Institute of Technology, Gulbahce, 35430 Urla, Izmir, Turkey

[3] Chronobiology unit, Groningen Institute for Evolutionary Life Sciences, University of Groningen, PO BOX 11103, 9700CC Groningen, Netherlands

[4] Centre for Biological Timing, Division of Diabetes Endocrinology and Gastroenterology, School of Medical Sciences, Faculty of Biology Medicine and Health, University of Manchester, Manchester M13 9PT, UK

* Equal contribution

Corresponding author

Abstract

Background

Light is a key environmental regulator of physiology and behaviour. Mistimed or insufficient light disrupts circadian rhythms and is associated with impaired health and well-being across mammals. Appropriate lighting is therefore crucial for indoor housed mammals. The most

commonly used measurement for lighting is lux. However, this employs a spectral weighting function based on human perceived brightness and is not suitable for 'non-visual' effects of light or use across species. In humans, a photoreceptor-specific (α-opic) metrology system has been proposed as a more appropriate way of measuring light.

Results

Here we establish technology to allow this α-opic measurement approach to be readily extended to any mammalian species, accounting for differences in photoreceptor types, photopigment spectral sensitivities, and eye anatomy. Since measuring photopigment spectral sensitivity can be hard to derive for novel animals and photoreceptors, we developed a high-throughput, easy-to-use, method to derive spectral sensitivities for recombinantly expressed melanopsins and use it to establish the spectral sensitivity of melanopsin from 12 non-human mammals. We further address the need for simple measurement strategies for species-specific α-opic measures by developing an accessible online toolbox for calculating these units and validating an open hardware, low-cost, multichannel light sensor for 'point and click' measurement. We finally demonstrate that species-specific α-opic measurements are superior to photopic lux as predictors of physiological responses to light in mice and allow ecologically relevant comparisons of photosensitivity between species.

Conclusion

Our study demonstrates that measuring light more accurately using species-specific α-opic units is superior to the existing unit of photopic lux and holds the promise of improvements to the health and welfare of animals, scientific research reproducibility, agricultural productivity, and energy usage.

Keywords: α-opic, light, irradiance, illuminance, photoreceptor, opsin, mammal

1. Background

Light is a crucial environmental factor that allows vision and plays a fundamental role in regulating physiological and behavioural processes(1). Light impacts animal biology by setting the phase of circadian rhythms and via direct effects on numerous aspects of behavioural and physiological state(2, 3). Understanding the effects of light on mammalian biology is therefore an important topic of research in its own right(4-7), while ensuring appropriate lighting is an important element of husbandry and a determinant of reproducible outcomes for common experimental paradigms(8-12). The most accessible method of measuring ambient light is to use a lux meter. These are widely obtainable and easy to use. Accordingly, light is commonly quantified in lux in animal research and husbandry(13-15). However, that approach is prone to error, as lux meters employ a light sensor and spectral filtering that match the spectral sensitivity of human flicker photometry (an assay of perceived brightness under cone-favouring conditions)(16). Given this narrow definition of spectral sensitivity, it is unsurprising that lights differing in spectral composition can have quite different impacts on animal biology even if matched for lux(17-19).

The challenge of achieving a wider quantification of ambient light than provided by a lux meter was recently addressed with publication of a new SI-compliant measurement system for light(20, 21). This new metrology aims to quantify light not in relation to its ability to elicit any particular biological response (e.g. perceived brightness in humans) but rather in terms of its effective intensity for each of the retinal photoreceptors responsible for detecting light.

In the case of humans, this allows quantification of 5 different 'α-opic irradiances' (rod-opic, melanopic, S-cone-opic, M-cone-opic, and L-cone-opic), corresponding to the effective irradiance for each of the 5 retinal photoreceptors in our own species(20). The definition of α-opic irradiance lends itself to adaption to other species. α-opic irradiance is calculated by weighting energy across the spectrum according to the wavelength sensitivity of the target photoreceptor. It follows that 'α-opic irradiance' may be calculated for any photoreceptor of known spectral sensitivity(20). Moreover, the α-opic standard encompasses an additional concept, that of 'equivalent daylight illumination' (EDI), which aides cross-species comparisons of light intensity. EDI is the quantity of daylight (in lux) required to produce the corresponding α-opic irradiance(22). A worked example illustrates how this facilitates ethologically relevant comparisons across species: say an experiment in mouse reveals impacts on learning at melanopic irradiance > 1 W/m^2. Expressing this in terms of melanopic EDI (>500 lux) introduces a relation to an environmental condition (an amount of daylight) which could be experienced by any species. If another study shows that in, say, horses effects on learning are observable only at >1000 lux melanopic EDI, then one could conclude that mice are twice as sensitive as horses to natural light and make precise predictions of the conditions under which light impacts learning in each species.

Although conceptually straightforward, there are currently several practical barriers to widespread adoption of the α-opic metrology across species. The first is incomplete knowledge of photoreceptor spectral sensitivity in some species. To calculate α-opic irradiance we need first to know what wavelength-dependent filter to apply, and this is defined by the wavelength sensitivity of that particular photoreceptor in that species. The second barrier is the absence of simple measurement methods (equivalent of a lux meter)

returning α-opic quantities. Here we address these problems. We describe an accessible method for determining unknown photoreceptor wavelength sensitivities and combine this with a review of published data to provide spectral sensitivity functions for calculating α-opic EDIs in major domestic mammal species. We provide an online resource for performing these calculations according to the methodology specified in CIE S026 and show that an open hardware multichannel light sensor can be used to quantify common light sources in α-opic metrics with reasonable accuracy.

2. Results

2.1. Defining photoreceptor spectral sensitivity

The α-opic metrology weights light energy across the spectrum according to the spectral sensitivity of each class of rod, cone or melanopsin photoreceptor. It follows that defining the spectral sensitivity of these photoreceptors in the target species is the critical step in adapting this approach to use across species. The photoreceptor spectral sensitivity itself is determined by two processes: the fundamental spectral efficiency of the photopigment responsible for light absorption; and the cumulative spectral filtering property of all elements upstream of that photopigment in the light path (pre-receptoral filtering).

A literature review reveals spectral sensitivity information is already available for many photoreceptors across mammalian species (**Supplementary table 1**). The primary exception is melanopsin, whose spectral sensitivity has so far been described in only a few instances. As

melanopsin is hard to purify in sufficient quantities for absorbance spectroscopy, we adapted a heterologous action spectroscopy method(23) to determine melanopsin spectral sensitivity for a wider array of species. In brief, HEK293T cells were transfected with an expression vector containing the cDNA sequence of the target melanopsin, presented with an appropriate isoform of retinal as chromophore, and the melanopsin-dependent light response was quantified using a luminescent reporter (**Figure 1A**). Luminescent response amplitude in this assay is dependent on the intensity and spectral composition of the stimulus, providing an opportunity to describe photopigment sensitivity as a function of wavelength(23). Here we exposed cells to 6 spectrally distinct stimuli over a range of irradiances (**Figure 1B**) and used a boot-strap modelling approach to determine the λ_{max} of a putative opsin photopigment which could best predict response amplitude across these stimuli (see methods). When applied to human melanopsin this method returned a λ_{max} estimate of 481 ±1.1nm, similar to published estimates for this species(23, 24) (**Figure 1D**). As a sense check, we confirmed the ability of a pigment with these characteristics to predict the luminescence responses, by plotting response amplitude as a function of effective irradiance for this pigment (weighting irradiance across the spectrum according to pigment sensitivity; **Figure 1E,F**). Having confirmed the suitability of this approach for human melanopsin, we tested it with 3 further melanopsins of known λ_{max} (mouse, crab-eating macaque, and brown rat). In each case our process returned λ_{max} ~480nm (mouse = 480±1.1nm; macaque = 483±1.2nm; rat = 481±1.1nm) (**Table 1; Supplementary table 2**), closely matching published spectral sensitivity estimates for melanopsin in these species(25-27).

Opsin photopigments can employ different *cis* isoforms of retinal as chromophore. As the identity of the isoform alters pigment λ_{max}, and as retinoids may be present in culture

143 medium, we finally wished to confirm that the outcome of our assay was determined by the
144 retinaldehyde added to the medium. To this end, we repeated the assay for our 4 test species
145 but adding 9- rather than 11-*cis* retinaldehyde to the culture medium. In other opsins, 9-*cis*
146 retinaldehyde causes a blue shift in spectral sensitivity(28), and this was also the case for
147 melanopsin with a mean±SD short wavelength shift of 16±2.5nm (range = 14 to 20nm) across
148 human, mouse, macaque and rat melanopsins (**Supplementary table 2**).
149
150 Having fully validated our approach, we turned to using it to define melanopsin spectral
151 sensitivity for 9 additional domestic mammalian species. To ensure consistency with future
152 work which may make use of commercially available 9-*cis* (in place of harder to obtain 11-*cis*)
153 retinaldehyde, we used the 9-*cis* chromophore for these experiments and applied a 16nm
154 correction. In all cases, the predicted λ_{max} for the 11-*cis* retinaldehyde photopigment was
155 close to 480nm (mean = 483nm; range 476-491nm; **Figure 1G**).
156
157 We next turned to the problem of how to account for the contribution of pre-receptoral
158 filtering on photoreceptor spectral sensitivity *in vivo*. In principle this can only be achieved by
159 measuring spectral transmittance of every element upstream of the photoreceptor in the
160 light path, or by describing the wavelength sensitivity of the target photoreceptor *in vivo*. The
161 latter approach has been used in a limited number of species for melanopsin but is not readily
162 applicable to new species. Turning to the former, we identified published reports of spectral
163 transmission for cornea, lens, and vitreous humor for seven mammalian species
164 (**Supplementary figure 1**). Each component of ocular media in all species had good
165 transmission across longer wavelengths. The extent of filtering at shorter wavelengths was
166 species-dependent and predominantly determined by the lens(18, 29). As lens transmission

is described for many mammalian species (**Supplementary data 1**) we wondered whether accounting for this parameter alone may adequately predict *in vivo* spectral sensitivity. To this end we identified species in which there was information available for lens transmittance; the absorbance spectrum of purified photopigment; and *in vivo* photoreceptor spectral sensitivity. In these cases, we calculated hypothetical *in vivo* photoreceptor λ_{max} as the product of photopigment *in vitro* spectral sensitivity and lens transmission. In all cases this estimated *in vivo* λ_{max} was similar to the experimentally measured value (**Supplementary table 1**) providing confidence that lens transmittance alone provides a reasonable approximation of pre-receptoral filtering in mammals. The literature contains information about lens transmission for at least 56 mammalian species, including humans (**Supplementary data 1**). The wavelength at 50% transmission (in which higher values represent low UV transmission), showed large interspecies variation, ranging from <310nm (European mole) to 494nm (European ground squirrel) (median 401.5 nm). It is well established that age can alter lens coloration and size, thereby modifying filtering properties(29). Thus, human pre-receptoral filtering standards are corrected for age(21). Given the challenges associated with accessing eyes of different ages from different species, we opted to perform our calculations using adult lens filtering for each species.

2.2. Calculation of species- and photoreceptor-specific light exposure metrics

Having determined methods for estimating *in vivo* spectral sensitivity we applied them to define functions for calculating α-opic irradiance for 12 domestic mammal species. The method of quantifying α-opic irradiance is captured by **equation 1** (**Table 2**) and relies on a full description of $s_{\alpha,s}(\lambda)$, the *in vivo* spectral sensitivity of the target photoreceptor (α) in

target species (s). We defined $s_{\alpha,s}(\lambda)$ for rod, cone and melanopsin photoreceptors across the 12 species of domesticated mammals by using the opsin template of Govardovskii and colleagues(30) and λ_{max} values from **Table 1** to produce a full *in vitro* spectral efficiency profile. We then multiplied by lens transmittance to provide $s_{\alpha,s}(\lambda)$, our estimate of *in vivo* spectral sensitivity for each pigment. Full functions for all pigments in all species are available in **Supplementary data 2A**.

Descriptions of α-opic irradiance for humans increasingly employ a derived quantity termed α-opic equivalent daylight illuminance (EDI)(31). EDI represents the illuminance (units = lux) of a standard daylight spectrum (termed D65) that would provide the equivalent α-opic irradiance. The method for calculating species-specific α-opic EDI (s α-opic EDI; e.g. 'mouse melanopic EDI'), involves first determining α-opic efficiency of D65 ($K_{\alpha,s,v}^{D65}$; W/lm) (**Table 2, Formula 2**) and then dividing α-opic irradiance ($E_{e,\alpha,s}$) by this value (**Table 2, Formula 3**). For simplicity, $K_{\alpha,s,v}^{D65}$ is provided for all target photoreceptors in **Supplementary data-2B**.

We provide two resources to facilitate calculation of species specific α-opic irradiance and EDI according to the equations in **Table 2** and the $s_{\alpha,s}(\lambda)$ functions in **Supplementary data 2**: an R package (alphaopics), which includes functions for calculating species and opsin-specific units (https://doi.org/10.48420/23283059); and an online toolbox (Alphaopics: Species-specific light exposure calculator) for easy calculation of species-specific metrics (https://alphaopics.shinyapps.io/animal_light_toolbox/). Both require the user to provide a measure of spectral power distribution ($E_{e,\lambda}(\lambda)$ for the light reaching the animal's eye.

2.3. Architecture for a miniaturised mammalian α-opic meter

Calculating α-opic quantities from full spectral power distributions requires an understanding of the properties of light and investment in appropriate measurement technology. For most users, a more 'point and click' solution to light measurement is required. Widely available lux meters already provide this when measuring photopic illuminance. Lux meters generally achieve the appropriate spectral weighting by combining the spectral sensitivity of the light sensor with an optic filter with an appropriate spectral transmission. Sadly, that strategy is not scalable for the α-opic metrology because, in principle, separate filters may be required for each potential target photoreceptor in each species. We wondered whether multichannel miniaturised (MM) light sensors could provide a solution to this problem and form the basis of easy-to-use light meters recording species specific α-opic units. MM sensors comprise 6 or more detectors, each sitting below an independent narrowband optical filter. They are relatively cheap, have high measuring accuracy of around 90% against calibrated sources, and have been used successfully to estimate human α-opic metrics(32-34). We set out to determine whether this technology could form the basis of accessible species-specific light meters. To this end, we attempted to recalibrate an open-source wearable light dosimeter (SpectraWear)(35) based upon a 10 channel MM sensor chip (AMS AS7341, Premstaetten, Austria) for species specific measurements.

To facilitate estimation of species- and photopigment-specific light exposures, we generated a set of narrow- and broad-band light stimuli with energy spanning the visible range (**Figure 2A**; see Methods). We then measured these with a spectroradiometer and applied the 'alphaopics' package to calculate species-specific α-opic EDIs. Next, we used nonlinear least-square fitting to derive weighting coefficients for the 10-channel sensor readings from

239 SpectraWear that best recreated the species-specific α-opic EDIs provided by those stimuli.
240 We finally validated the resulting calibration coefficients against a test set of lights generated
241 from the narrow- and broad-band sources used for calibration but spanning a wider range of
242 irradiances. A comparison of measured (based upon full spectral power density
243 measurements) and predicted (based upon SpectraWear) EDIs showed strong correlations for
244 all α-opic irradiances in a single representative species (**Figure 2B**). To provide a more
245 comprehensive description of the device performance across α-opic quantities and species,
246 we calculated the estimation error (difference between measured and predicted α-opic EDI)
247 for each test stimulus for the α-opic quantities of our 12 domestic mammal species and
248 humans (**Figure 2C)**. This revealed variations in performance across different α-opic
249 quantities, with consistently high accuracy for melanopic and rhodopic EDIs for all species
250 evaluated (**Figure 2C**; typical estimation errors = 0.06±0.01 & 0.05±0.01 log units respectively;
251 median±SD). Despite the substantial variation in cone opsin λ_{max} across species, L- and M-
252 cone opic EDIs were also estimated with good reliability (**Figure 2D**; typical estimation errors
253 = 0.06±0.02 log units). Conversely, performance was reduced for S-cone-opic EDIs, especially
254 in species where S-cones show peak sensitivity in the UV (**Figure 2D**; typical estimation errors
255 = 0.30±0.45 log units). In sum, the performance of the device allowed us to reconstruct
256 reliable estimates (within ±17%) of α-opic EDIs other than S-cone opic. This technology could
257 enable continuous light monitoring in field with a scalable design.
258
259 **2.4. Characterisation of species-specific light exposure amongst common illuminants**
260
261 We finally turned to describing the suitability of the α-opic metrology for predicting the
262 response of animals to light of divergent spectral composition. In the first instance we asked

whether α-opic units predicted responses within a single candidate species to spectrally divergent stimuli. That is a prerequisite for using any metric to standardise husbandry or recreate experimental conditions. Many studies of circadian photoentrainment in mice quantify light in photopic lux. We took four datasets describing irradiance response curves for circadian phase shifting in wild-type and retinal degenerate mice across the wavelength range(36-38) and expressed them either as a function of photopic lux, or the mouse α-opic EDIs (**Figure 3A, B, Supplementary figure 2A-C**). We found that the fraction of variance in circadian phase shift predicted by light intensity (R^2 for curve fit) was >0.8 when light intensity was quantified in any of mouse melanopic, rhodopic or M-cone-opic EDIs but substantially reduced when either photopic lux (0.4) or S-cone opic EDI (0.2) were used (**Figure 3C**). This finding highlights the superior capacity of the α-opic metrology to predict mouse circadian phase resetting to spectrally divergent lights.

We wondered the extent to which this improvement relied upon adoption of species-specific metrics or whether human α-opic units would achieve the same effect. To this end, we generated versions of the mouse irradiance response curves with light intensity expressed in human α-opic units. As there is great cross-species divergence in spectral sensitivity of cone photoreceptors, it is perhaps unsurprising that human L/M-cone-opic EDIs provided an inadequate prediction of the mouse response (**Figure 3C**). The reduction in goodness of fit when expressing light in human melanopic or rhodopic EDI is less expected given the similarity in spectral sensitivity of melanopsin and rod opsin photopigments across mammals. However, there is substantial divergence in lens transmission to short wavelength light across these species. Accordingly, an assessment of relative melanopic sensitivity for mouse vs human as a function of wavelength (**Figure 3C**) reveals that, while the two species have very similar

sensitivity >450nm, their sensitivity to shorter wavelengths diverges. It follows that human quantities may be more appropriate for lights that lack strong output at very short wavelengths (as is the case for most artificial sources). We tested this prediction by excluding data for UV wavelengths from our phase shift dataset and recalculating goodness of fit to human melanopic and rhodopic EDI. In both cases the human metrics now provided goodness of fit for the mouse phase shifting irradiance response curve (**Figure 3C**). Together these analyses reveal the advantages of using species-specific versions of the α-opic units, while showing that there may be circumstances (melanopic and rhodopic EDIs for stimuli with little UV output) under which human metrics are an acceptable alternative.

Having confirmed the advantages of the α-opic metrology for predicting the animal response to light, we quantified the potential error associated with the current practice of quantifying light in photopic lux. An appropriate measurement system should allow the animal's experience of lights differing in spectral composition to be normalised. We therefore took α-opic EDI as a measure of true effective intensity and asked how well the current practice of using measuring light in photopic lux predicted α-opic EDI. We started with the most widely encountered case of broad-spectrum lights of the types used for general illumination applications. Taking 42 such broad-spectrum lights, intensity matched for photopic lux (and thus under current practice considered to be interchangeable for animal work), we calculated their α-opic EDI for each of the 13 mammals. This revealed substantial variation in effective intensity for each photoreceptor (α-opic EDIs) across the various light sources. Shown for a representative species (mouse) in **Figure 4A** left. At the extreme, two broad-spectrum lights, intensity matched in photopic lux, could show 85% difference in melanopic EDI. The poor

suitability of the photopic lux metric for predicting α-opic EDI was even starker for monochromatic or 'coloured' lights (**Figure 4A** right).

Thus far, we have considered the advantages of the α-opic EDI metrology for quantifying effective intensity for different light sources within a species. A further aspect of the metrology is its ability to allow informative comparisons of light intensity between species, e.g., to ask whether some species are fundamentally more sensitive to light than others. The α-opic EDI concept incorporates an anchor to the natural world (an equivalent amount of daylight), which should facilitate ecologically relevant comparisons cross-species. To illustrate this, **Figure 4B** shows a plot of the relationship between solar angle and human melanopic irradiance for a range of real-world light measures. The nature of the correction used to convert α-opic irradiance to EDI ensures that this relationship is near identical for all α-opic EDIs across all species ($r>0.99$). It follows that lights of equivalent α-opic EDI should recreate each animal's experience of a similar solar angle with good accuracy even across species. To confirm this, we calculated the solar angle corresponding to 1000 lux melanopic EDI in each of 13 mammalian species (humans + the 12 domesticated mammals defined above). The result is plotted in **Figure 4C** and confirms that in all species this recreates the experience of natural light when the sun is just above the horizon. For comparison we estimated the appropriate solar angle for our 42 broad-spectrum lights when set to 1000 photopic lux (by converting to melanopic EDI and relating to the function in **Figure 4B**). In this case, the equivalent solar angle became more variable, encompassing sunrise and much of the civil twilight range (**Figure 4C).**

3. Discussion

No animal is equally sensitivity to light at all wavelengths. It follows that applying the appropriate spectral weighting function is critical in quantifying light in photobiology. The α-opic concept of light measurement was first proposed in 2014 to account for the then still quite recent discovery of the inner retinal photoreceptor melanopsin, and the related realisation that lights matched for photopic illuminance could have quite divergent ability to elicit important circadian and neurophysiology light responses(20). The α-opic metrology has a quite different conceptual basis than conventional photometry. Whereas photopic illuminance quantifies light according to the spectral sensitivity of a single distinct percept (perceived brightness under cone favouring conditions), the α-opic metrology aims to quantify light according to the experience of each photoreceptor type, remaining agnostic to its final application in supporting vision or reflex light responses. What is lost in simplicity is gained in flexibility. Thus, while the single measure of photopic lux is replaced by 5 α-opic irradiances (for humans), the latter capture all relevant information about incident light, whereas the former only captures information about its perceived brightness. The additional flexibility of the α-opic metrology is especially valuable when quantifying light for non-human animals. Most mammals lack the long-wavelength shifted L/M cones that dominate the photopic sensitivity function in humans(19). Replacement spectral efficiency functions for perceived brightness are not readily obtainable for many species and in any case would not capture important circadian and neurophysiological light responses. By contrast, information about photoreceptor spectral sensitivity is often available, allowing species specific α-opic functions to provide a holistic description of the animal's experience of light. This ability of the α-opic metrology to provide species-specific quantification of light was recognised in the

356 initial description of the approach and yet, while α-opic units are now increasingly presented
357 in the context of human light exposure(31) they have not been widely adopted for non-human
358 animals. There are likely several reasons for this. Most importantly, a push for more
359 widespread appreciation of this strategy has awaited formal specification of the α-opic
360 approach as an internationally approved standard metrology. With that in place, more
361 practical problems about how to measure species-specific α-opic units come into focus. Here
362 we have addressed two of these: gaps in our knowledge of photoreceptor spectral sensitivity
363 for some species; and a high barrier to entry for those wishing to measure light in this way.
364 Having addressed these, we provide some simulations to quantify the advantages of applying
365 α-opic units in animal biology.
366
367 Our approach to filling gaps in knowledge of photoreceptor spectral sensitivity has been to
368 employ a heterologous action spectroscopy approach, which we first used to study human
369 melanopsin(23). We have adapted that strategy to make it higher throughput by optimising
370 the range of wavelengths/irradiances used and by applying a bootstrap modelling approach
371 to analysis which provides the optimal pigment λ_{max} for the data collected and an error
372 estimate for that value. The result is a relatively high-throughput method, requiring little
373 specialist lab equipment and applicable to any photoreceptor with known cDNA sequence.
374 We have applied it to define melanopsin spectral sensitivity because, while other methods
375 (electroretinography or microspectrophotometry) are available for rods and cones in
376 domestic mammals, studying melanopsin *in vivo* is more challenging(27, 39). In principle the
377 method could be applicable to any photoreceptor from any species for which a live cell
378 readout of photoactivation is available. One important consideration in these data is that
379 cDNA sequences for melanopsin are not available for many species. In these instances,

predicted coding sequences for genomic data have been used, with the associated potential for errors(40, 41). Indeed, when aligning melanopsin sequences against the confirmed sequence for humans, several sequences listed on databases were missing key regions due to mis-identified splicing. It is for this reason that we did not rely upon one gene database for the generation of melanopsin sequences.

Our data reveal conservation of melanopsin spectral sensitivity across the 13 mammalian species described here. The total range of predicted λ_{max} is 15nm, which is similar to that for rod opsin across these species (13nm), but small compared to that of either S- or M-cones (>50nm). The fact that the species showing greatest difference in melanopsin λ_{max} are both small diurnal mammals from semi-arid environments (striped mouse and mongolian gerbil) adds to the impression that this parameter is not under divergent selection pressure across the species studied here. An interesting question is what features of the light environment and/or structural contraints for the protein may be responsible for restricting melanopsin λ_{max} to ~480nm.

Opsin photopigments can employ a range of cis- isoforms of retinaldehyde as chromophore, and in the case of melanopsin there is evidence of diversity in the choice of isoform *in vivo*. As opsin spectral sensitivity is influenced by the retinaldehyde isoform used, it is important to note that the values presented here represent those with the 11-cis isoform of A1 retinaldehyde. The resultant estimates for spectral sensitivity match those for whole animal responses in mice, macaque and humans. The reader is directed elsewhere for a complete consideration of factors determining estimates of melanopsin spectral sensitivity in other elements of the literature(42).

In principle, the method of calculating α-opic EDI is applicable to any photoreceptor from any species. In the case of mammals, future work may extend it to Opn5 and/or Opn3 as further evidence of their sensory functions accumulates, although careful consideration of appropriate pre-receptoral filtering is required for opsins expressed outside of the eye(43-45). The number of α-opic EDIs required to fully quantify the light environment for many non-mammalian species may be large, as these commonly have many photopigment types expressed in different parts of the body (and thus subject to divergent pre-receptoral filtering). Nevertheless, calculating these quantities would represent an advance on alternatives that either assume equal sensitivity across the spectrum (unweighted sum of energy/quanta) or human spectral sensitivity (photopic illuminance).

Spectrometers capable of providing spectral power density measures, which in combination with a suitable wavelength weighting function can be used to calculate species-specific α-opic metrics, are widely available. The toolbox presented here to facilitate this process represents an extension on previously published versions restricted to a smaller number of species(17, 20, 46, 47). More accessible 'point and click' solutions to calculate species specific units could take advantage of meters recently developed to measure human α-opic metrics. In particular, we show here that appropriate calibration allows the MM technology forming the basis of several such meters to measure many species specific quantities with acceptable accuracy (<17% error rate). We validate an approach based upon a system developed an open hardware principles (Spectrawear(35)), but commercially available products could in principle be adapted to this purpose. One important caveat here is that core MM chips generally do not have good coverage at short wavelengths (especially UV) over which many domestic

mammals are much more sensitive than humans(18, 48). That likely explains the poor performance of Spectrawear for S-cone opic EDI and suggests that meters including separate UV sensitive detector(s) could have superior performance.

Quantifying light in species-specific α-opic EDI has clear conceptual advantages over current practices of using either photopic illuminance or total energy/quanta. We show here that it also provides superior ability to predict circadian phase shift responses in mice (across numerous studies) and allows sensible comparisons of effective light intensity across species. Application of this metrology could thus bring coherence to the growing literature on light effects on mammalian physiology and behaviour and reproducibility to any experiment in which light influences the outcome. Appropriate measurement can also have a wider significance for animal welfare. Insufficient daytime light and excessive light at night have been shown to disrupt circadian rhythm and sleep, and have negative impacts on the health of animals, as well as research outputs and scientific reproducibility(4-12). Animal-centered approaches are key to enhancing the health and wellbeing of indoor housed animals, and the accurate provision of light is a crucial consideration. Environmental light pollution poses a significant disruptor to many animal ecosystems, emphasizing the need for better characterization of animal-specific light exposure to improve conservation strategies(49, 50). Furthermore, given the significant land and energy usage required for farm animal operations, the identification of optimum lighting conditions that balance productivity, health, and electricity usage has the potential to generate substantial energy savings(51-53). Additionally, the impact of evening and night-time light exposure in the home environment on human sleep is well-documented(54), but remains unknown for pets(55). One process that could facilitate these applications would be simplification of the 4 α-opic quantities required to fully

describe irradiance for most mammalian species to a single metric that provides a reasonable prediction of light responses of interest under most circumstances. This could be a single α-opic metric or a composite of several. Such a process has led to the increasing use of melanopic EDI as a single metric for non-visual light responses in humans(31).

4. Conclusions

Our study reveals an accessible method to measure photopigment-specific "α-opic" light exposure for mammal species. We present the prerequisite data for defining α-opic metrics; lens transmission, and novel action spectra for melanopsins from most major domesticated mammalian species. We then present the necessary calculations to derive photoreceptor-specific metrics and provide open access software for easy calculation. Our data reveals that species-specific α-opic metrics offer greater accuracy for the description of the physiological effects of light than the current commonly used standard of photopic lux. Finally, we present a prototype low-cost and scalable portable light dosimeter for the measurement of lighting conditions. This method for light measurement allows for the easy monitoring, regulation and intervention of light exposure in animal housings and will lead to increased research accuracy using animal models, agricultural efficiency and improve animal health and wellbeing.

5. Methods

5.1. Recombinant cloning of animal opsins

Coding sequences for mammalian melanopsins were accessed from either NCBI GenBank or Ensembl databases (Ensembl Release 109(56)). Open reading frames for the following sequences were used to construct expression vectors: brown rat Opn4, NM_138860.1; cat

476 Opn4, NM_001009325.2; cattle Opn4, NM_001192399.1; crab-eating macaque Opn4,
477 ENSMFAT00000002526.2; dog Opn4, XM_038662366.1; four-striped grass mouse Opn4, in
478 house cDNA; horse Opn4, XM_023648726.1; human OPN4, NM_033282.4; Mongolian gerbil
479 Opn4, XM_021635996.1; mouse Opn4L, NM_013887.2; Rabbit Opn4,
480 ENSOCUT00000017574; Sheep Opn4, XM_027962232.2; Syrian hamster Opn4,
481 ENSMAUT00000015782 (**Supplementary table 3, 4**). Gene sequences were synthesised using
482 ThermoFisher GeneArt Gene Fragment synthesis and TwistBio Gene Fragment synthesis and
483 underwent codon optimisation where necessary for synthesis. All opsin sequences were
484 tagged with the 1D4 epitope (TETSQVAPA) on the C-terminus. Opsins were introduced into
485 the multiple cloning site of the pcDNA3 vector (Invitrogen) downstream of the CMV promoter
486 using NEBuilder HiFi Assembly (New England Biolabs).
487
488 **5.2. Heterologous action spectroscopy**
489 HEK293T cells (American Type Culture Collection) were cultured in Dulbecco's modified
490 Eagle's Medium (4.5 g l−1 D-glucose, sodium pyruvate and L-glutamine with 10% foetal calf
491 serum; DMEM). Cells were transiently transfected with 500ng plasmid expression vectors for
492 the relevant opsin and 500ng genetically encoded Ca^{2+} indicator mtAequorin (as described in
493 (23)) using lipofectamine 2000 (Invitrogen) and incubated overnight with 10µM 9-*cis*-retinal
494 (Sigma-Aldrich) or 10uM 11-*cis*-retinal (National Eye Institute, National Institutes of Health).
495 The following day, cells were incubated with 10µM Coelenterazine-h (Promega) in the dark
496 for 2 hours before recording luminescence in a plate reader (Optima FLUOStar, BMG)
497 modified to allow "In-well" stimulation with an external light source (CoolLED pe-4000,
498 CoolLED) via fibre optic. Luminescence recordings were sampled at a temporal resolution of
499 2 seconds per timepoint. Baseline luminescence was recorded for 10 seconds, after which

cells were stimulated with light (1s duration) of varying intensities (11 – 16 log photon/cm^2/sec total photon flux) at one of 6 different wavelengths (435nm, 460nm, 470nm, 490nm, 500nm, 525nm).

5.3. Calculation of opsin photon sensitivity peaks

To determine the λ_{max} values for each opsin, we employed a nonlinear optimization strategy. In this strategy, an optimization algorithm systematically iterates over different values of λ_{max} (*optim* function in *R* (version 4.3.0), using the Brent search method). Each iteration consisted of two steps. First, the effective photon flux values of the light sources were updated according to the Govardovskii photopigment template(30) corresponding to the currently assumed value for λ_{max}. Then, a 5-parameter log-logistic model was fitted with cell response and the updated effective photon flux as dependent and independent variables respectively (*drm* function from the *drc* package (version 3.0-1)), from which the estimation error was extracted (i.e., residual sum of squares). The optimization algorithm searched for the λ_{max} value (within a 400-600 nm range) that would minimize this error. Finally, bootstrapping was performed in which the above optimization procedure was repeated 1000 times, each time using only a random subset of the data (with replacement). The average and standard deviation of the 1000 resulting λ_{max} values were finally used as the λ_{max} estimate and estimation error.

5.4. Standardization of animal lens transmissions

Literature searches for lens, cornea, and vitreous humor light transmissions for mammal species were performed. We accessed data from 56 adult species. References and data are listed in **Supplementary data 1**. Human pre-receptoral filtering is based on a reference

observer of age 32 years(20, 21). If available in the reference source table or supplement, original data was used. Otherwise, data was extracted from reference plot using WebPlotDigitizer (Version 4.6). If relative absorbance was reported, transmission was calculated as $100 \times 10^{-Relative\ absorbance}$. To harmonize the data the following steps were performed. If less than 50 data points available, cubic splines with 1 nm step were interpolated. If more than 50 data points available, smoothing splines with 1 nm step and 50 knots were interpolated. All raw data were normalized to their maximum values (max. 100%). Data were filled with the last value until 800 nm and were filled until 310 nm using the slope of the first 3 values. Negative values were accepted as zero. Where multiple valid sources were available (e.g., Syrian hamster and Brown rat), mean fits were used. For seven species (European ground squirrel, Syrian hamster, thirteen-lined ground squirrel, coruro, Mongolian gerbil, seal, cattle) cornea or vitreous humor filtering information were available. For those, we compared the wavelength where transmission reached 50% in lens, cornea, and vitreous humor. Lens transmission for European ground squirrel (Spermophilus citellus) and Syrian hamster were measured as previously described(57), for tree shrew (Tupaia belangeri) and Fat-Tailed Dunnart (Sminthopsis crassicaudata) an AvaSpec 2048 (Avantes) UV/VIS spectrometer with a perpendicular fibreoptics transmission setup was used.

5.5. Prototyping of a mammal light dosimeter and its calibration

The prototype is based on an open-access human α-opic light dosimeter electronic design(35). The device prototype of 3D-printed black plastic outer case, micro SD card memory storage and Bluetooth control. The device light detection had transparent acrylic disc (Perspex) with 20mm diameter and with a diffuser (Optsaver L-35 Kimoto, Cedartown, Georgia, USA) underneath. The device incorporates AMS AS7341 multichannel spectral colour

548 sensor (ams, Premstaetten, Austria), which had channels having peak wavelengths at 415nm,
549 445nm, 480nm, 515nm, 555nm, 590nm, 630nm, 680nm, 910nm, and a clear channel to read
550 unfiltered spectral input. Sensor reading of a prototype device were collected across 169 light
551 conditions (13 distinct spectra across multiple irradiances). This included ten distinct
552 narrowband spectra, generated via a calibrated multispectral LED light source (CoolLED pE-
553 4000 LED Illumination System; narrowband peaks: 405, 435, 460, 470, 490, 500, 525, 550,
554 595, 635 and 660nm) and three distinct broadband spectra (Philips CorePro white LED 470
555 lumen 4000K, Philips Tornado white fluorescent 1570 lumen 2700K or CoolLED pE-4000 LED
556 Illumination System 365-460-525-635nm colour-mixed white LED) Throughout, stimuli were
557 measured via a calibrated spectroradiometer (SpectroCal, Cambridge Research Systems, UK)
558 and converted to species specific α-opic EDIs as described above. All measurements were
559 performed in a dark room. We then collected an identical set of measurements of the same
560 stimuli user our 10-channel light sensor (integration time 182ms, automatic gain optimisation
561 in the range of 8 – 512X and additional post hoc scaling by a factor of 10^6 such that sensor
562 counts took on positive values >=1). To calibrate the device, we then selected a subset of 3
563 measurements for each of the 13 distinct spectra described above. Based on the known
564 relationship between the measured sensor counts and the α-opic irradiance of these
565 calibration stimuli (and our previous observations that these sensors exhibit good linearity
566 across a very wide range(35)), we extrapolated the expected sensor counts for each spectra
567 across a consistent set of EDI values (-1, 0.5 and 2 log lux). We then fit a set of weighting
568 coefficients such that the sum of the adjusted log sensor counts best recreated the expected
569 log EDIs across stimuli in the calibration dataset (using 'lsqcurvefit' function in Matlab R2018a,
570 Mathworks, MA, USA). We choose to perform fits on log transformed data since this allowed
571 for sensor weightings to be either positive or negative (important for reliable estimates from

572 low channel count sensors such as this) while avoiding the possibility that any resulting
573 estimated α-opic EDI might take on (impossible) negative values. To validate the resulting
574 species- and photoreceptor-specific device calibration, we then used the derived sensor
575 weighting coefficients to estimate EDIs across the remaining 130 spectroradiometrically
576 measured test stimuli that didn't contribute to calibration (n=3-27 irradiances/spectrum at
577 unweighted irradiances of ~0.2-80W/m^2). Log (absolute) errors for these estimates, relative
578 to the directly measured values, were then determined for each distinct spectrum, species
579 and photopigment.
580
581 **5.6. Characterisation of species-specific light exposure amongst common illuminants**
582 We selected four datasets(36-38) including more than five light stimuli with different spectral
583 distributions. Phase shift values were extracted from graphs using WebPlotDigitizer (Version
584 4.6) and light stimuli spectral power distributions were generated as normal distribution with
585 specified peak wavelength and half width at half maximum values (Matlab R2018a,
586 Mathworks, MA, USA). We then converted them to human photopic lux, the mouse α-opic
587 EDIs and the human α-opic EDIs. We fitted non-linear four-parameter lines to estimate phase
588 shifts using light stimuli.
589
590 All test light sources were arbitrarily set to 100 human photopic lux. Indoor artificial standard
591 illuminants included: CIE standard illuminant A (incandescent 2855 K), CIE standard illuminant
592 HP types (High pressure sodium lamps 1-5; standard, colour-enhanced, metal halide), CIE
593 standard illuminant FL types (Fluorescent 1-12 and 3.1-3.15; standard, broad-band, narrow-
594 band, standard halophosphate, DeLuxe type, three-band, multi-band, D65 simulator), CIE
595 standard illuminant LED types (Light-emitting diode B1-B5, BH1, RGB1 and V1-V2; Phosphor-

type LEDs with different correlated colour temperatures, Hybrid-type, RGB-type, and violet-pumped phosphor-types)(58, 59). As narrowband test light source, we measured spectral power distributions of CoolLED pE-4000 LED Illumination System (narrowband peaks: 365, 405, 435, 470, 500, 525, 550, 595, 635) using a spectroradiometer (SpectroCal, Cambridge Research Systems, UK). For 13 species which we have both opsin sensitivity and lens transmission information (Human, mouse, four-striped grass mouse, brown rat, Syrian hamster, Mongolian gerbil, cattle, sheep, horse, cat, dog, crab-eating macaque, rabbit), α-opic EDIs were calculated. Using GraphPad Prism 9, between-species mean and range were plotted for each light source.

Natural daylight spectral irradiances, solar angle (degree) and weather conditions on multiple days were collected in the University of Groningen, the Netherlands (latitude: 53.24°, longitude: 6.54°)(60). Daylengths at the measurement date were calculated using R package 'suncalc' (0.5.1). We used a subset of the data (−6° to 60° solar angle, weather conditions >6 cloudy or <3 clear, summer daylengths >15h). In total, our data included 5 days of clear sunny conditions (4633 measurements) and 11 days of overcast daylight (10433 measurements). Human and mouse melanopic EDIs (mean $\pm$ range) were plotted against solar angle. For 13 species, α-opic EDIs representing that solar angle were calculated and compared pairwise using Pearson correlation. Finally, above mentioned CIE light sources matched for either 1000 human photopic lux or species-specific melanopic EDI lux (for 13 species). These values were converted to solar angles using the above mentioned curves.

6. List of Abbreviations

9-*cis* – 9-*cis* retinaldehyde

620 11-*cis* – 11-*cis* retinaldehyde

621 λ_{max} – The wavelength at which maximum activity/absorption occurs

622 EDI - equivalent daylight illumination

623 MM light sensor - multichannel miniaturised light sensor

624 UV - Ultraviolet

625

626 **7. Declarations**

627 **Ethics approval and consent to participate**

628 Transmission data was collected under the University of Groningen Animal Experiments
629 Committee license number BG02197/98.

630

631 **Consent for publication**

632 Not applicable.

633

634 **Availability of data and materials**

635 The datasets generated and/or analysed during the current study are available in the
636 following Figshare repository: https://doi.org/10.48420/23708610. Functions for calculating
637 the Functions for calculating species and opsin-specific units are available as an R package
638 (alphaopics) (https://doi.org/10.48420/23283059); and an online toolbox (Alphaopics:
639 Species-specific light exposure calculator) for easy calculation of species-specific metrics
640 (https://alphaopics.shinyapps.io/animal_light_toolbox/).

641

642 **Competing interests**

643 RJL and TMB have received investigator-initiated grant funding from Signify/Philips Lighting
644 and RJL has received honoraria from Samsung Electronics. RJL has received a financial support
645 from NASA, UFAW (11-22/23) and the University of Manchester to organize a workshop about
646 the measurement of species-specific light units for laboratory mammals (Manchester, 2023).
647

648 **Funding**

649 This work was funded by a Wellcome Trust Investigator Award (210684/Z/18/Z) and European
650 Research Council (951644-SOL) to RJL.
651

652 **Author's contributions**

653 RJM and RJL designed the opsin sensitivity measurement methodology, and RJM and MJG
654 performed the photopigment sensitivity experimental measurements. AD searched literature
655 for prereceptoral filtering data. RJM searched literature for spectral sensitivities. RAH
656 performed novel transmission measurements. AD, RJM, TW and TMB performed data
657 analysis. TMB, RJL and AD were involved in the design, production and calibration of the light
658 dosimeters. AD, TW, RJM and RJL drafted the manuscript. TMB, RJL, AD and RJM were
659 involved in planning and supervising the project. All authors discussed the results and
660 commented on the manuscript. All authors have read and agreed to the final manuscript.
661

662 **Acknowledgements**

663 We thank Lucien Bickerstaff for his help in calibration of the light dosimeter. We also thank
664 Prof Ron Douglas (City University London) for his guidance on lens transmission of mammals.
665

8. References

1. Vetter C, Pattison PM, Houser K, Herf M, Phillips AJK, Wright KP, et al. A review of human physiological responses to light: implications for the development of integrative lighting solutions. Leukos. 2021;18(3):387-414.

2. Campbell I, Sharifpour R, Vandewalle G. Light as a Modulator of Non-Image-Forming Brain Functions-Positive and Negative Impacts of Increasing Light Availability. Clocks Sleep. 2023;5(1):116-40.

3. Duffy JF, Czeisler CA. Effect of Light on Human Circadian Physiology. Sleep Med Clin. 2009;4(2):165-77.

4. Bano-Otalora B, Martial F, Harding C, Bechtold DA, Allen AE, Brown TM, et al. Bright daytime light enhances circadian amplitude in a diurnal mammal. Proc Natl Acad Sci U S A. 2021;118(22).

5. Dauchy RT, Wren-Dail MA, Hoffman AE, Hanifin JP, Warfield B, Brainard GC, et al. Effects of Daytime Exposure to Light from Blue-Enriched Light-Emitting Diodes on the Nighttime Melatonin Amplitude and Circadian Regulation of Rodent Metabolism and Physiology. Comp Med. 2016;66(5):373-83.

6. Lucassen EA, Coomans CP, van Putten M, de Kreij SR, van Genugten JH, Sutorius RP, et al. Environmental 24-hr Cycles Are Essential for Health. Curr Biol. 2016;26(14):1843-53.

7. Tam SKE, Brown LA, Wilson TS, Tir S, Fisk AS, Pothecary CA, et al. Dim light in the evening causes coordinated realignment of circadian rhythms, sleep, and short-term memory. Proc Natl Acad Sci U S A. 2021;118(39).

687 8. Aulsebrook AE, Jechow A, Krop-Benesch A, Kyba CCM, Longcore T, Perkin EK, et al.
688 Nocturnal lighting in animal research should be replicable and reflect relevant ecological
689 conditions. Biol Lett. 2022;18(3):20220035.
690 9. Nelson RJ, Bumgarner JR, Liu JA, Love JA, Melendez-Fernandez OH, Becker-Krail DD,
691 et al. Time of day as a critical variable in biology. BMC Biol. 2022;20(1):142.
692 10. Prager EM, Bergstrom HC, Grunberg NE, Johnson LR. The importance of reporting
693 housing and husbandry in rat research. Front Behav Neurosci. 2011;5:38.
694 11. Steel LCE, Tir S, Tam SKE, Bussell JN, Spitschan M, Foster RG, et al. Effects of Cage
695 Position and Light Transmission on Home Cage Activity and Circadian Entrainment in Mice.
696 Front Neurosci. 2021;15:832535.
697 12. Emmer KM, Russart KLG, Walker WH, Nelson RJ, DeVries AC. Effects of light at night
698 on laboratory animals and research outcomes. Behav Neurosci. 2018;132(4):302-14.
699 13. The Welfare of Farmed Animals (England) Regulations 2000. 2000.
700 14. Directive 2010/63/EU of the European Parliament and the Council of 22 September
701 2010 on the protection of animals used for scientific purposes. 2010.
702 15. Code of Practice for the Housing and Care of Animals Bred, Supplied or Used for
703 Scientific Purposes. 2014.
704 16. ISO/CIE DIS 23539:2021(E): Photometry – The CIE system of physical photometry.
705 2021.
706 17. Peirson SN, Brown LA, Pothecary CA, Benson LA, Fisk AS. Light and the laboratory
707 mouse. J Neurosci Methods. 2018;300:26-36.
708 18. Hut RA, Kronfeld-Schor N, van der Vinne V, De la Iglesia H. In search of a temporal
709 niche: environmental factors. Prog Brain Res. 2012;199:281-304.

19. Hagen JFD, Roberts NS, Johnston RJ. The evolutionary history and spectral tuning of vertebrate visual opsins. Developmental Biology. 2023;493:40-66.

20. Lucas RJ, Peirson SN, Berson DM, Brown TM, Cooper HM, Czeisler CA, et al. Measuring and using light in the melanopsin age. Trends Neurosci. 2014;37(1):1-9.

21. CIE S026/E:2018: CIE System for Metrology of Optical Radiation for ipRGC-Influenced Responses to Light. 2018.

22. Brown TM. Melanopic illuminance defines the magnitude of human circadian light responses under a wide range of conditions. J Pineal Res. 2020;69(1):e12655.

23. Bailes HJ, Lucas RJ. Human melanopsin forms a pigment maximally sensitive to blue light (λmax ≈ 479 nm) supporting activation of Gq/11 and Gi/o signalling cascades. Proceedings of the Royal Society B: Biological Sciences. 2013;280(1759):20122987.

24. Gamlin PDR, McDougal DH, Pokorny J, Smith VC, Yau K-W, Dacey DM. Human and macaque pupil responses driven by melanopsin-containing retinal ganglion cells. Vision Research. 2007;47(7):946-54.

25. Berson DM, Dunn FA, Takao M. Phototransduction by Retinal Ganglion Cells That Set the Circadian Clock. Science. 2002;295(5557):1070-3.

26. Lucas RJ, Douglas RH, Foster RG. Characterization of an ocular photopigment capable of driving pupillary constriction in mice. Nature Neuroscience. 2001;4(6):621-6.

27. Liu A, Milner ES, Peng YR, Blume HA, Brown MC, Bryman GS, et al. Encoding of environmental illumination by primate melanopsin neurons. Science. 2023;379(6630):376-81.

28. Sekharan S, Morokuma K. Why 11-cis-Retinal? Why Not 7-cis-, 9-cis-, or 13-cis-Retinal in the Eye? Journal of the American Chemical Society. 2011;133(47):19052-5.

733 29. Douglas RH, Jeffery G. The spectral transmission of ocular media suggests ultraviolet
734 sensitivity is widespread among mammals. Proc Biol Sci. 2014;281(1780):20132995.
735 30. Govardovskii VI, Fyhrquist N, Reuter T, Kuzmin DG, Donner K. In search of the visual
736 pigment template. Vis Neurosci. 2000;17(4):509-28.
737 31. Brown TM, Brainard GC, Cajochen C, Czeisler CA, Hanifin JP, Lockley SW, et al.
738 Recommendations for daytime, evening, and nighttime indoor light exposure to best
739 support physiology, sleep, and wakefulness in healthy adults. PLoS Biol.
740 2022;20(3):e3001571.
741 32. Mohamed A, Kalavally V, Cain SW, Phillips AJK, McGlashan EM, Tan CP. Wearable
742 light spectral sensor optimized for measuring daily α-opic light exposure. Opt Express.
743 2021;29(17):27612-27.
744 33. Amirazar A, Azarbayjani M, Molavi M, Karami M. A low-cost and portable device for
745 measuring spectrum of light source as a stimulus for the human's circadian system. Energy
746 and Buildings. 2021;252:111386.
747 34. Stampfli JR, Schrader B, di Battista C, Häfliger R, Schälli O, Wichmann G, et al. The
748 Light-Dosimeter: A new device to help advance research on the non-visual responses to
749 light. Lighting Research & Technology. 2023:14771535221147140.
750 35. Mohammadian N, Didikoglu A, Beach C, Wright P, Mouland JW, Martial F, et al. A
751 wrist worn Internet-of-Things sensor node for wearable equivalent daylight illuminance
752 monitoring. TechRxiv. 2023.
753 36. Yoshimura T, Ebihara S. Spectral sensitivity of photoreceptors mediating phase-shifts
754 of circadian rhythms in retinally degenerate CBA/J (rd/rd) and normal CBA/N (+/+)mice. J
755 Comp Physiol A. 1996;178(6):797-802.

37. van Oosterhout F, Fisher Simon P, van Diepen Hester C, Watson Thomas S, Houben T, VanderLeest Henk T, et al. Ultraviolet Light Provides a Major Input to Non-Image-Forming Light Detection in Mice. Current Biology. 2012;22(15):1397-402.

38. Hattar S, Lucas RJ, Mrosovsky N, Thompson S, Douglas RH, Hankins MW, et al. Melanopsin and rod-cone photoreceptive systems account for all major accessory visual functions in mice. Nature. 2003;424(6944):76-81.

39. Emanuel AJ, Do MT. Melanopsin tristability for sustained and broadband phototransduction. Neuron. 2015;85(5):1043-55.

40. van den Burg MP, Vieites DR. Bird genetic databases need improved curation and error reporting to NCBI. Ibis. 2023;165(2):472-81.

41. Goudey B, Geard N, Verspoor K, Zobel J. Propagation, detection and correction of errors using the sequence database network. Briefings in Bioinformatics. 2022;23(6).

42. Emanuel AJ, Do MTH. The multistable melanopsins of mammals. Frontiers in Ophthalmology. 2023;3.

43. Nayak G, Zhang KX, Vemaraju S, Odaka Y, Buhr ED, Holt-Jones A, et al. Adaptive Thermogenesis in Mice Is Enhanced by Opsin 3-Dependent Adipocyte Light Sensing. Cell Reports. 2020;30(3):672-86.e8.

44. Buhr ED, Yue WWS, Ren X, Jiang Z, Liao H-WR, Mei X, et al. Neuropsin (OPN5)-mediated photoentrainment of local circadian oscillators in mammalian retina and cornea. Proceedings of the National Academy of Sciences. 2015;112(42):13093-8.

45. Rao S, Chun C, Fan J, Kofron JM, Yang MB, Hegde RS, et al. A direct and melanopsin-dependent fetal light response regulates mouse eye development. Nature. 2013;494(7436):243-6.

779 46. Enezi J, Revell V, Brown T, Wynne J, Schlangen L, Lucas R. A "melanopic" spectral
780 efficiency function predicts the sensitivity of melanopsin photoreceptors to polychromatic
781 lights. J Biol Rhythms. 2011;26(4):314-23.
782 47. Allen AE, Mouland JW, Rodgers J, Bano-Otalora B, Douglas RH, Jeffery G, et al.
783 Spectral sensitivity of cone vision in the diurnal murid Rhabdomys pumilio. J Exp Biol.
784 2020;223(Pt 11).
785 48. Jacobs GH, Neitz J, Deegan JF, 2nd. Retinal receptors in rodents maximally sensitive
786 to ultraviolet light. Nature. 1991;353(6345):655-6.
787 49. Gaston KJ, Duffy JP, Gaston S, Bennie J, Davies TW. Human alteration of natural light
788 cycles: causes and ecological consequences. Oecologia. 2014;176(4):917-31.
789 50. Jägerbrand AK, Bouroussis CA. Ecological Impact of Artificial Light at Night: Effective
790 Strategies and Measures to Deal with Protected Species and Habitats. Sustainability.
791 2021;13(11).
792 51. Lee K, Elliott C, Pattison PM. Energy Savings Potential of SSL in Agricultural
793 Applications. 2020.
794 52. Lindkvist S, Ternman E, Ferneborg S, Bankestad D, Lindqvist J, Ekesten B, et al. Effects
795 of achromatic and chromatic lights on pupillary response, endocrinology, activity, and milk
796 production in dairy cows. PLoS One. 2021;16(7):e0253776.
797 53. Lutzer A, Nagel C, Murphy BA, Aurich J, Wulf M, Gautier C, et al. Effects of blue
798 monochromatic light directed at one eye of pregnant horse mares on gestation, parturition
799 and foal maturity. Domest Anim Endocrinol. 2022;78:106675.
800 54. Cain SW, McGlashan EM, Vidafar P, Mustafovska J, Curran SPN, Wang X, et al.
801 Evening home lighting adversely impacts the circadian system and sleep. Sci Rep.
802 2020;10(1):19110.

803 55. Houpt KA, Erb HN, Coria-Avila GA. The Sleep of Shelter Dogs Was Not Disrupted by
804 Overnight Light Rather than Darkness in a Crossover Trial. Animals (Basel). 2019;9(10).
805 56. Cunningham F, Allen JE, Allen J, Alvarez-Jarreta J, Amode M R, Armean Irina M, et al.
806 Ensembl 2022. Nucleic Acids Research. 2021;50(D1):D988-D95.
807 57. Hut RA, Scheper A, Daan S. Can the circadian system of a diurnal and a nocturnal
808 rodent entrain to ultraviolet light? Journal of comparative physiology A. 2000;186(7-8):707-
809 15.
810 58. CIE 015:2018: Colorimetry, 4th Edition. 2018.
811 59. ISO/CIE 11664-2:2022(E): Colorimetry — Part 2: CIE standard illuminants. 2022.
812 60. Woelders T, Wams EJ, Gordijn MCM, Beersma DGM, Hut RA. Integration of color and
813 intensity increases time signal stability for the human circadian system when sunlight is
814 obscured by clouds. Sci Rep. 2018;8(1):15214.
815
816

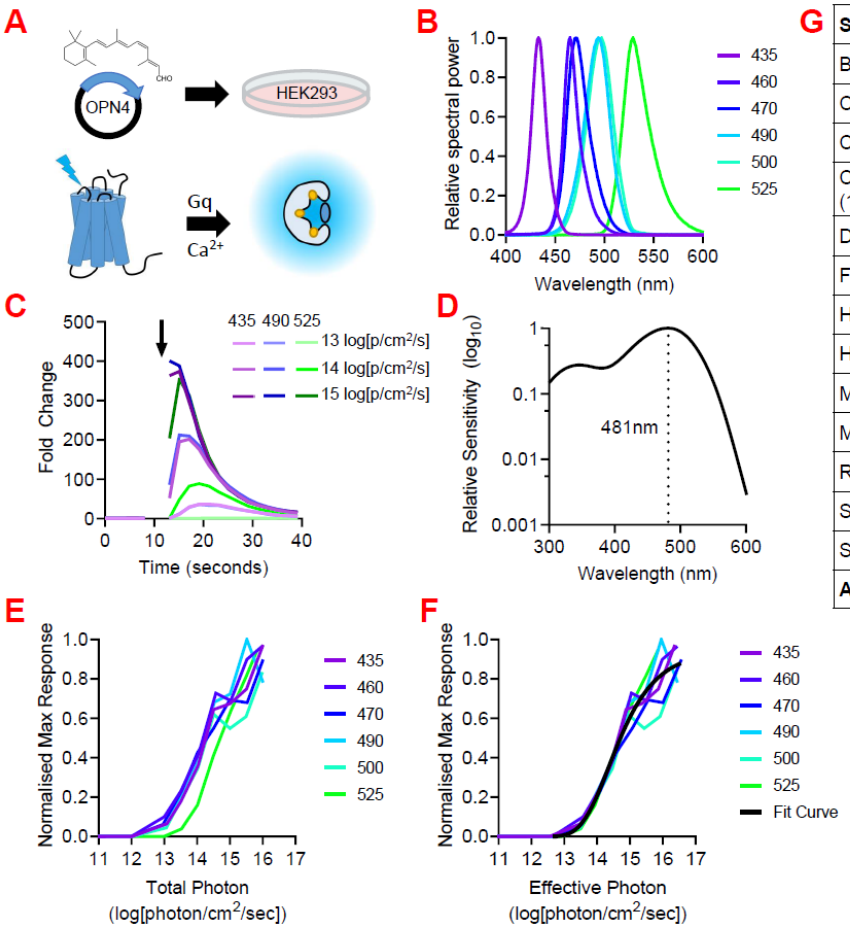

G

Species	λ_{max}	SD
Brown rat (11-cis)	481	1.1
Cat	488	1.0
Cattle	484	1.1
Crab-eating macaque (11-cis)	483	1.2
Dog	488	0.9
Four-striped grass mouse	476	0.9
Horse	482	0.9
Human (11-cis)	481	1.1
Mongolian gerbil	491	1.0
Mouse (11-cis)	480	1.1
Rabbit	488	0.7
Sheep	484	1.1
Syrian hamster	479	0.7
Average	483	

Figure 1: Mammalian melanopsin spectral sensitivities. (**A**) Schematic of action spectra generation. HEK293 cells are incubated with 11-*cis* or 9-*cis* retinal and transfected with plasmid DNA containing melanopsin from the species of interest. Light stimulation drives an increase in intracellular Ca^{2+} via Gq pathway activation, which causes bioluminescence from the Ca^{2+} indicator mtAequorin. Bioluminescence is detected by a plate reader. (**B**) Spectra of stimulating lights used to generate action spectra. (**C**) Example time course showing changes in hOPN4-mediated increases in Ca^{2+} bioluminescence under different stimulating light spectra and intensities. (**D**) Example Govardovskii template for hOPN4 based on predicted λ_{max} 481nm. (**E**) Example irradiance response curves (IRCs) for hOPN4 plotted against uncorrected total photon light intensity. (**F**) Example irradiance response curves (IRCs) for hOPN4 plotted against corrected effective photon light intensity weighted for a photopigment with λ_{max} 481nm. (**G**) Predicted λ_{max} of mammalian melanopsins. Data collected with 9-*cis* retinal and subsequently scaled to λ_{max} for 11-*cis* retinal, unless labelled with '(11-*cis*)', indicating data was collected with 11-*cis* retinal.

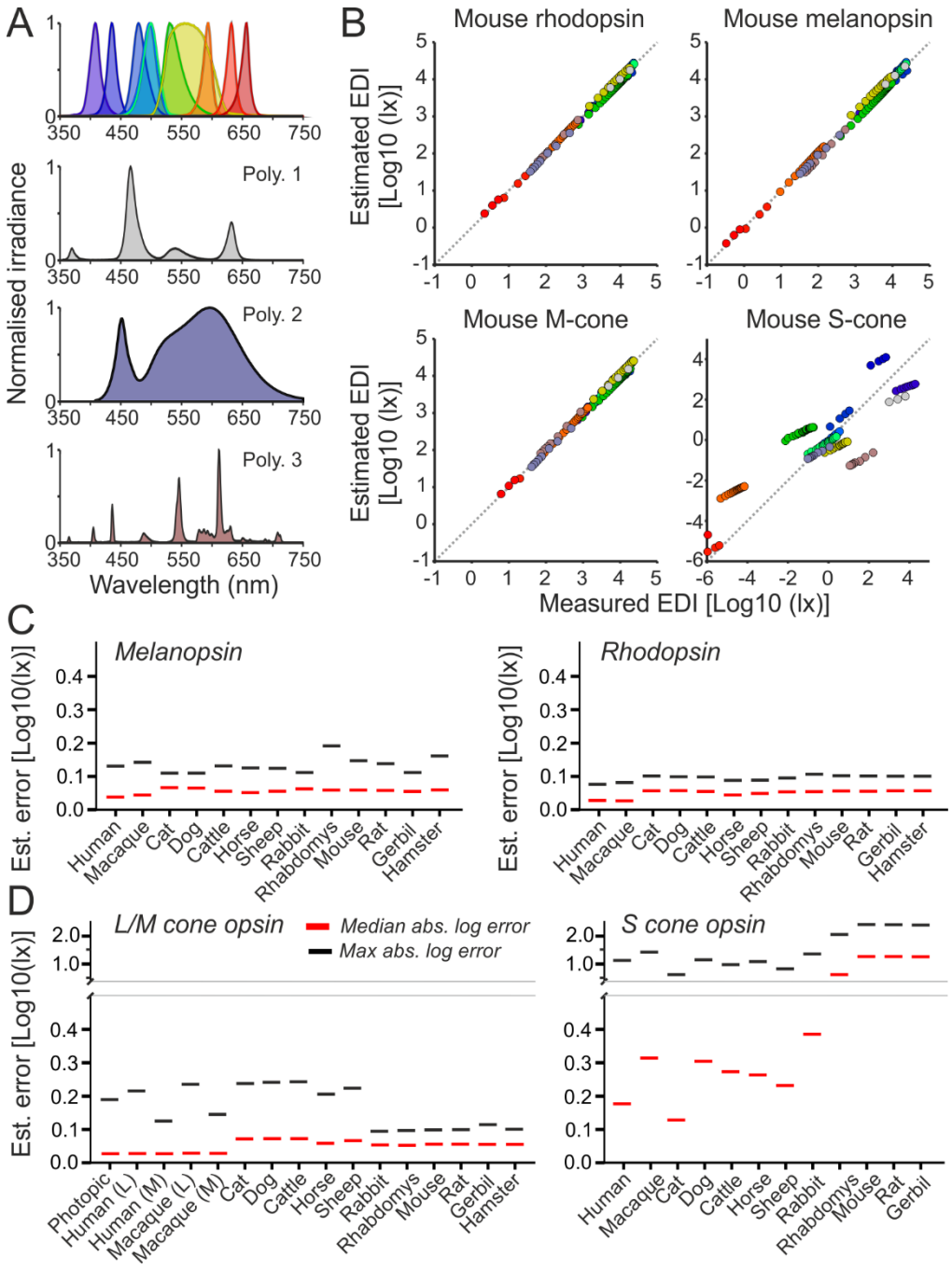

Figure 2: Cross-species light dosimeter validation. (**A**) Normalised spectral power distributions of ten narrow- (top) and three broadband stimuli (lower panels) used for device calibration and validation. (**B**) Top panels show scatter plots of relationship between mouse α-opic EDIs, determined based on spectroradiometric measurements, for stimuli in A across a range of irradiances and the corresponding estimated melanopic EDIS based on weighted readings from the 10-channel light sensor. (**C,D**) Plots showing median and maximum log absolute errors for melanopic (**C**, left), rhodopic (**C**: right), L/M-cone opic (**D**, left) and S-cone opic (**D**, right) EDIs across species.

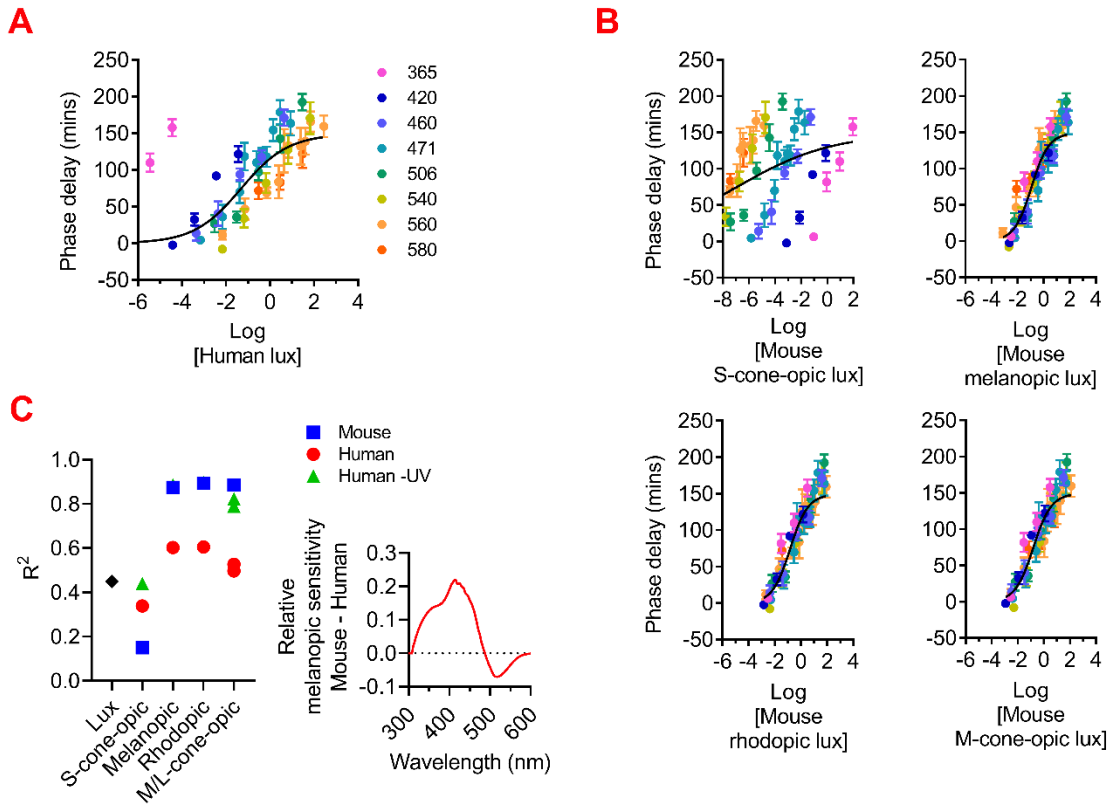

Figure 3: Irradiance response curves for circadian phase shifting in C57 wild-type mouse(37). Phase delays (mean±SEM) were plotted against eight narrowband light stimuli with a range of intensities. Light stimuli were presented as human photopic lux in (**A**), mouse α-opic EDIs in (**B**). Non-linear four-parameter fit lines were shown in all plots. R^2 for curve fits were shown in (**C**). In addition to mouse-specific α-opic EDIs, curve fits for human α-opic EDIs were also presented (with and without light stimuli at 365nm). Lower right plot shows comparison of relative melanopic sensitivity for mouse vs human as a function of wavelength.

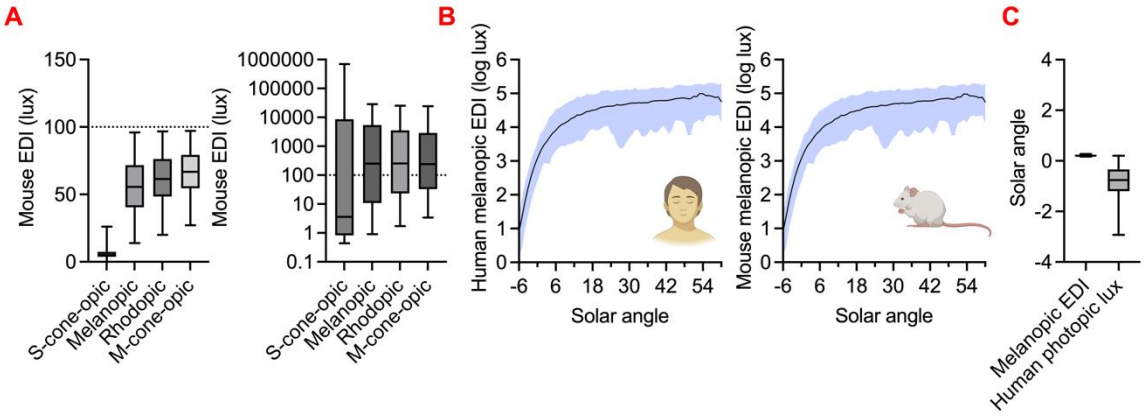

Figure 4: Cross-species α-opic EDIs across different light sources. (**A**) Comparison of mouse α-opic EDIs across (left, linear Y-axis) 42 broad-spectrum CIE standard white light sources and (right, log-scale Y-axis) 9 monochromatic LED light sources matched for 100 human photopic lux. Box plots show mean and ranges. (**B**) Plots of the relationship between solar angle and human (left) and mouse (right) melanopic EDIs for a range of real-world light measures. Natural spectral irradiances over 16 days were collected in the Netherlands (latitude: 53.24°, longitude: 6.54°, summer daylengths >15h) and comprises overcast and clear weather conditions shown with error range(60). (**C**) White light sources in **A** were converted to species-specific melanopic EDIs for 13 species reported in this study. Box plots show mean±range of solar angle that represent either 1000 species-specific EDI lux or 1000 human photopic lux matched light inputs.

870 **Table 1:** List of mammal photopigment spectral sensitivities

Species	**Species (latin name)**	**S-cone-opsin λ_{max}**	**Melanopsin λ_{max}**	**Rhodopsin λ_{max}**	**M-cone-opsin λ_{max}**	**L-cone-opsin λ_{max}**
Mouse	Mus musculus	358	480	498	508	---
Four-striped grass mouse	Rhabdomys pumilio	360	476	493	501	---
Brown rat	Rattus norvegicus	358	481	498	509	---
Syrian hamster	Mesocricetus auratus	---	479	502	504	---
Mongolian gerbil	Meriones unguiculatus	360	491	502	490	---
Cattle	Bos taurus	435	484	500	553*	---
Sheep	Ovis aries	440*	484	500[#]	549*	---
Horse	Equus ferus caballus	428	482	499	545	---
Cat	Felis catus	450	488	501	553	---
Dog	Canis lupus familiaris	428*	488	506	554*	---
Rabbit	Oryctolagus cuniculus	421*	488	502	509	---
Crab-eating macaque	Macaca fascicularis	415	483	500	535	567

[#] Accepted Rod 500nm

* Adjusted for lens transmission because the raw data come from *in vivo* ERG

References and measurement method in **Supplementary table 1**

Human photopigment spectral sensitivities are based on the CIE metrics for non-visual human light exposure(21): S-cone-opic 447nm, melanopic 488nm, rhodopic 504nm, M-cone-opic 540nm, L-cone-opic 565nm.

871

872

873

874

875

876

877

878 **Table 2:** Formulas used to calculate species and photopigment-specific light exposure metrics

1	Species-specific α-opic irradiance	$E_{e,\alpha,s} = \int E_{e,\lambda}(\lambda) s_{\alpha,s}(\lambda) d\lambda$
2	Species-specific α-opic efficacy of luminous radiation	$K_{\alpha,s,v}^{D65} = \frac{E_{e,\alpha,s}^{D65}}{E_{v}^{D65}}$
3	Species-specific α-opic equivalent daylight illuminance	$E_{v,\alpha,s}^{D65} = \frac{E_{e,\alpha,s}}{K_{\alpha,s,v}^{D65}}$

879

880

881 **Additional Files**

882 Supplementary Table 1: Literature search for opsin spectral sensitivities in the absence of

883 prereceptoral filtering.

884 Supplementary table 2: Different isoforms of retinal in measurements of OPN4 spectral

885 sensitivities (λmax).

886 Supplementary table 3: Amino acid sequences of mammalian melanopsins used in study.

887 Supplementary table 4: Nucleotide sequences of mammalian melanopsins used in study.

888

889 Supplementary data 1: Literature search for lens transmission for 56 mammalian species.

890

891 Supplementary data 2A: Estimation of *in vivo* spectral sensitivity for each photopigment for

892 each mammalian species.

893 Supplementary data 2B: α-opic efficiency of D65 ($K_{\alpha,s,v}^{D65}$; W/lm) for each photopigment for all

894 target species.